

Fixed value from Table 2.  
Assumed values (see text).

Case	$K_0$	$M_b$	$K_0$	$(\alpha K_0 / \alpha T)^p$	$\gamma$	$d \ln Y$	$d \ln V$
1	1.27	5.6	-0.05	0.43	-0.04	4.9	6.4
2	1.36	4.1	-0.05	0.46	1.2	4.6	6.6
3	0.974	7.3	-0.05	0.33	-0.15	6.15	6.4

TABLE 6. Coesite Parameters for Various Cases

pressures, but this scatter would only cause in the points is due to the scatter in Hugoniot in the previous sections. A greater uncertainty by using the different equations of state given by this pressure, the difference between pressures are due to the change by only a few percent at 2.3  $M_b$  is over 30,000°K. The term-point is over 40,000°K and that the  $P_c = 1.77$  point is 7 and 8). It is notable that the 5.5-Mb (Figures 7 and 8). It is also notable that the results are plotted against Hugoniot pressure according to the method described earlier. The by Truini *et al.* [1971b], have been calculated properties, which were calculated approximately For detailed comparison the Hugoniot temperature phases are equal at the phase transition. condition that the Gibbs free energies of the as a function of temperature by using the two-phase transition can be calculated as shown in Figure 3. But the discrete energy calculations of state just given, the discrete-energy calculations of state of state just given, By using the equations of state given, the Gibbs free energies of coesite and stishovite-vitre can now be calculated, and the coesite-stishovite transition pressure can be calculated 1.35 g/cm<sup>3</sup>. Hugoniot data are considerably scattered and that they do not trend toward the coesite density of 2.91 g/cm<sup>3</sup>, perhaps because these points, the other excluding them.

### SiO<sub>2</sub>: Phase Equilibrium

What uncorrected at this stage. They cannot definitely be said to be discordant with case 3, but the discrepancy between cases with some equation of state of coesite must remain significant. Because of this discrepancy, the equilibrium of the stishovite phase. When they are compared to the  $P_c = 1.15$  g/cm<sup>3</sup> Hugoniot data, the cause there has been a partial conversion to the stishovite phase. When they are compared to the coesite density of 2.91 g/cm<sup>3</sup>, perhaps because these points, the other excluding them, were taken from the Debye model.

The scatter in their interpretation are such that most of the corresponding Hugoniot data.

The scatter in the Hugoniot data and the most of the Hugoniot data given [1970] very well, and it falls below and Basnett [1970] not fit the static-compression data of Basnett 6). It can be seen (Figure 6) that case 3 does not fit the compression data (Table 6 and Figure 6). The bulk modulus in Figure 6 and Figure 6 is fixed at this value and only  $K_0$ , determined 1972), and so a third case was run with  $K_0$ , et al. (H. Mizutani, private communication 1977). This value was run with  $K_0$  measured ultrasonically by Mizutani 0.97 Mb measured ultrasonically by Mizutani two cases are significantly above the value of case 2 in Figure 6. The bulk modulus in these given in Table 5. Case 1 is illustrated in Figure I, case 2 in Table 5. Case 1 is illustrated in Figure 6, cases 1 and case 2 including them. The standard points used to weight the compression data are errors and case 2 including them. The standard points and case 2 in Table 1 and 2 in Table 6, cases 1 excluding the three doubtful Hugoniot points are given as cases 1 and 2 in Table 6, the results are static-compression data. The Hugoniot results and static-compression data, finally both  $K_0$  and  $K_c$ , were determined three points, the other excluding them.

It can be seen from Figure 1 that the  $P_c = 1.15$  g/cm<sup>3</sup> Hugoniot data are considerably scattered from the Debye model. The values of  $V$  and  $C_v$  were taken from Table 2, and  $C_p$ , was calculated from the Debye model.

Data	$M_b$	Error,
S11	0.20	0.02
S12	0.10	0.10
S13	0.10	0.10
X3		

TABLE 5. Standard Errors Assumed for the Coesite, Compression Data

Because of the smaller range and quantity

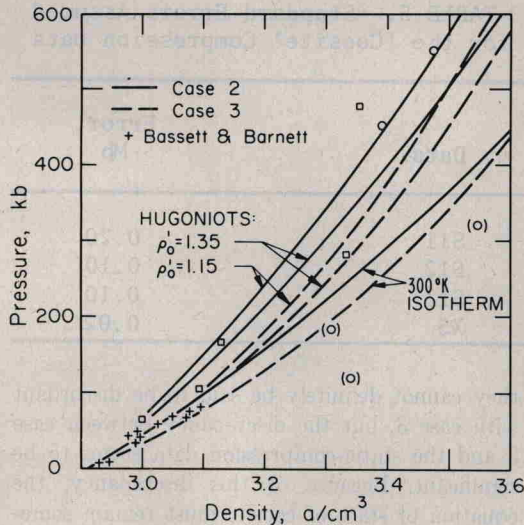


Fig. 6. Hugoniot data of 'coesite' and calculated Hugoniots and 300°K isotherms from cases 2 and 3 (Table 6). Symbols are those used in Figures 1 and 5.

the points to move along the Hugoniot locus, which in a  $P$ - $T$  plot is approximately radial from the initial point.

The boundary between the 'coesite' and stishovite fields (Figure 8) is closely defined by the  $\rho_0' = 1.77$  and  $\rho_0' = 1.55 \text{ g/cm}^3$  Hugoniot points, both of which show signs involving a mixture of the two phases, as was discussed earlier.

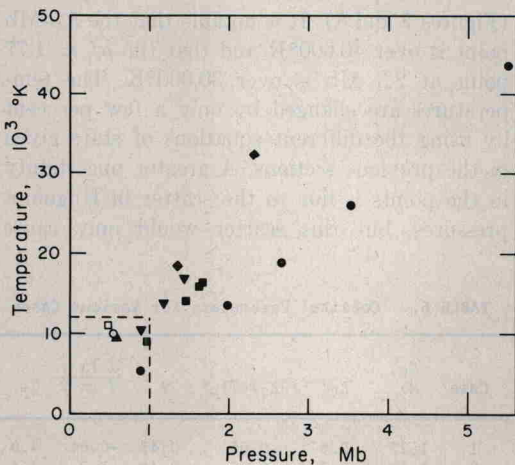


Fig. 7. Calculated Hugoniot temperatures of stishovite and 'coesite' versus Hugoniot pressure. Box is enlarged in Figure 8. Symbols are those used in Figure 1.

The Gibbs free energy is defined by

$$G = H - TS = U + PV - TS \quad (14)$$

where  $H$  is the enthalpy and  $S$  is the entropy. Here  $G$  has the property [e.g., Slater, 1939]

$$(\partial G / \partial P)_T = V \quad (15)$$

We wish to evaluate  $G$  at the state  $(P, V, T)$ , starting from the state  $(0, V_0, T_0)$ . (Atmospheric pressure can be ignored here.) This evaluation will be done via the state  $(P_0, V_0, T)$ , where  $P_0(T) = P(V_0, T)$  (i.e., by first raising the temperature at constant volume and then compressing isothermally). From (14)

$$\begin{aligned} G(V_0, T) &= G(V_0, T_0) \\ &+ [U(V_0, T) - U(V_0, T_0)] + P_0(T)V_0 \\ &- [TS(V_0, T) - T_0S(V_0, T_0)] \end{aligned} \quad (16)$$

and from (15), upon integration,

$$G(V, T) = G(V_0, T) + \int_{P_0(T)}^{P(T)} V(P', T) dP' \quad (17)$$

When the difference between the Gibbs free energies of stishovite and coesite at the state  $(V_0, T_0)$  are denoted by  $\Delta G_0$  (i.e.,

$$\Delta G_0 = G^s(V_0^s, T_0) - G^c(V_0^c, T_0)$$

where superscripts  $s$  and  $c$  denote stishovite and

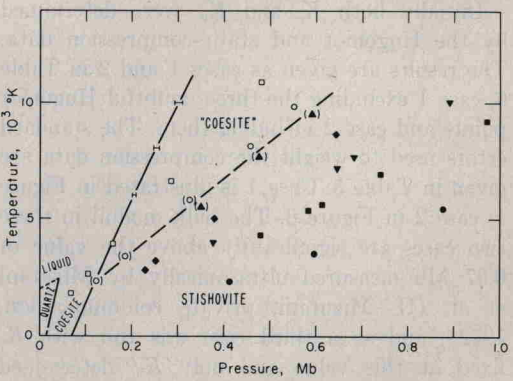


Fig. 8. Calculated Hugoniot temperatures of stishovite and 'coesite' versus Hugoniot pressure compared with observed and calculated (solid and short-dashed) phase lines. Long-dashed line separates stishovite and 'coesite' fields. Error bars represent variations due to the use of alternative equations of state given in previous sections. Symbols are those used in Figure 1.